The effect of copper on the selective carbon monoxide oxidation over alumina supported gold catalysts

Thiago S. Mozer, Dominika A. Dziuba [1], Carlos T.P. Vieira, Fabio B. Passos [*]

Departamento de Engenharia Química e de Petróleo, Universidade Federal Fluminense (UFF), Niterói, RJ, Brazil

ABSTRACT

The selective oxidation of CO in the presence of H_2 was investigated on Au catalysts promoted with different amounts of Cu. Au catalysts were prepared by the deposition–precipitation method and exhibited a satisfactory activity at low temperature with adequate selectivity. A considerable improvement in CO conversion was achieved when the O_2/CO ratio was increased from the value of 0.5–1.0. The addition of Cu to Au/Al_2O_3 catalysts caused an increase in the selectivity to CO oxidation due to an interaction between Au and Cu on the surface of the catalysts. However, this beneficial effect was limited to an optimal content of Cu. The catalysts were characterized by temperature programmed reduction and DRS UV–vis spectroscopy, indicating the formation of small bimetallic Au–Cu particles. The presence of water vapor in the feed stream played a positive effect in the CO conversion and selectivity while the CO_2 presence diminished the CO conversion and selectivity. In the case of a realistic reformate, when both H_2O and CO_2 are present, the positive effect of H_2O was able to compensate the negative effect of CO_2 depending on the temperature of reaction.

© 2008 Elsevier B.V. All rights reserved.

1. Introduction

Fuel cells are a promising alternative for energy generation due to their higher energy efficiency as compared to conventional combustion engines. Fuel cells are a clean technology, with very low pollutant emission [1,2]. In particular, the polymer electrolyte membrane fuel cell (PEMFC) has been considered suitable for vehicles and portable applications. PEMFC uses hydrogen as fuel, but its Pt electrode is severely poisoned by the presence of carbon monoxide even in low concentrations (10 ppm) [3–5]. As the main process for generation of hydrogen is the steam reforming of hydrocarbons, hydrogen produced is contaminated with carbon monoxide. Selective carbon monoxide oxidation is one of the most promising methods to reduce carbon monoxide content in the hydrogen feed to acceptable levels [1,6], but hydrogen oxidation competes with carbon oxidation, leading to fuel loss.

Gold was considered a catalytic inert material, until the discovery that Au nanoparticles of less than 5 nm in diameter were active for CO oxidation at low temperatures [7]. Additionally, the rate of CO oxidation on supported Au catalysts was higher than the observed for H_2 oxidation [8]. This is a prerequisite for the selective oxidation of CO in H_2 rich gas streams at temperatures corresponding to the operating temperature of PEMFC [9]. There's been quite a debate in the literature about the nature of the catalytic sites of supported gold catalysts. For example, Haruta and co-workers [10] attributed the Au catalytic activity to the presence of metallic gold. However, Park and Lee [11] reported that oxidized gold species were more active than metallic gold and Fierro-Gonzalez et al. [12] showed evidence that cationic gold plays a role both in the presence and in the absence of metallic gold. Costello et al. [13] attributed the catalytic activity to an ensemble of metallic Au atoms and a cationic Au with a hydroxyl group. Gold catalytic activity is related to the metal particle size generated during the catalyst preparation [14]. Catalysts with particle sizes around 5–10 nm showed better activity and selectivity [15]. In this case, low coordinated edge and corner Au atoms are present, and the number of such atoms on the metal surface was found to correlate with catalytic activity [16].

Few studies dealt on the addition of promoters to gold catalysts used in the selective CO oxidation. The addition of Ba to gold was found to be beneficial in keeping the particle size small; favoring the activity of CO oxidation, while the addition of Ce has not affected the catalytic performance [17]. In the case of Pt–Au catalysts, the existence of an optimal Pt–Au ratio for the selective CO oxidation was observed [18]. Chimentão et al. [19] studied $Au–Cu/TiO_2$ catalysts for propene epoxidation and demonstrated the existence of Au–Cu

* Corresponding author at: Rua Passo da Pátria 156, Niterói 24210-240, RJ, Brazil. Tel.: +55 21 26295599; fax: +55 21 26295368.

E-mail addresses: thiagomozer@yahoo.com.br (T.S. Mozer), d.dziuba@gmx.de (D.A. Dziuba), tadeupadilha@hotmail.com (C.T.P. Vieira), fbpassos@vm.uff.br (F.B. Passos).

[1] Permanent address: Hochschule Mannheim (HS), Mannheim, BW, Germany.

alloy particles (5–15 nm) which were more active than monometallic Au or Cu samples. Cu was able to modify the reactivity of Au and seemed to have a strong influence on the dispersion and catalytic properties decreasing the metal particles sizes. Thus, the variation of Au surface structure by the presence of copper could be beneficial to the selective CO oxidation. In fact, Au–Cu/SBA-15 were shown to be active in CO oxidation in the presence of hydrogen, but the effect on selectivity was not discussed [20] In this work, the effect of Cu addition on Au/Al$_2$O$_3$ used in the CO selective oxidation was investigated. We have examined how copper and gold bimetallic particles behave in terms of CO oxidation activity and selectivity in the presence of H$_2$. Additionally, we have studied the effect of O$_2$ content, as well as the influence of the presence of H$_2$O and CO$_2$ in the reactant stream on the activity and selectivity of the catalysts.

2. Experimental

2.1. Catalyst preparation

The catalysts were prepared by the deposition–precipitation method, which is considered the most suitable method to prepare gold catalysts [21]. HAuCl$_4$ (Aldrich, 99,999%) and CuCl$_2$·2H$_2$O (Merck, 99%) were used as precursors. The support (γ-Al$_2$O$_3$) was obtained by calcination of bohemite at 550 °C for 2 h.

An aqueous solution of HAuCl$_4$ at pH 8 was added with vigorous stirring to a suspension of γ-Al$_2$O$_3$ and deionized water at room temperature. A NaOH aqueous solution was used to keep the solution at pH 8 and to minimize the presence residual chloride [22]. Residual chloride can poison the active site by displacing the hydroxyl group and it also induces agglomeration of gold particles [13]. In the case of the bimetallic catalysts, a CuCl$_2$ aqueous solution was added to the suspension. The suspension was stirred for 2 h and then vacuum filtered. It was next washed twice with deionized water, followed by drying at 120 °C for 16 h. In order to minimize possible light-sensitive reactions of the Au precursor, the synthesis was carried out with minimal exposure to light. Additionally, the catalysts were not calcined in order to avoid the sinterization of gold particles during the thermal treatment.

Cu/Al$_2$O$_3$ was prepared by incipient wetness, using CuCl$_2$·H$_2$O as precursor (Merck, 99%). This sample was dried at 120 °C for 16 h and calcined at 500 °C for 2 h.

2.2. Catalyst characterization

2.2.1. BET surface area

BET surface areas were determined by nitrogen adsorption at 77 K in a Micromeritcs ASAP 2010 automated gas sorption analyzer. The pretreatment of the samples (1 g) consisted of drying under vacuum at 150 °C for 3 h.

2.2.2. Temperature programmed reduction (TPR)

TPR experiments were performed in a multipurpose unit coupled to a mass spectrometer (Balzers Omnistar). The catalysts (500 mg) were dried in He for 30 min at 150 °C before TPR analysis. After cooling to room temperature, a mixture of 5% H$_2$ in Ar flowed through the sample at 30 mL min^{-1}, and the temperature was raised at a heating rate of 10 °C min^{-1} up to 1000 °C.

2.2.3. UV–vis diffuse reflectance spectroscopy (DRS UV–vis)

The UV–vis diffuse reflectance spectroscopy was performed in air using a Varian Cary 500 spectrometer. The DRS spectra were obtained by subtraction of Al$_2$O$_3$ spectra from the corresponding Au and Au–Cu/Al$_2$O$_3$ spectra. Reflectance data were converted to pseudo-absorbance by using the Kubelka-Munk formalism.

2.2.4. Selective CO oxidation

For selective CO oxidation, 200 mg of catalyst was placed in a glass microreactor. The reactant feed consisted of 1% CO; 0.5–1.5% O$_2$; 30% H$_2$; 0–30% CO$_2$; 0–10% H$_2$O and He balance, depending on the desired conditions. The total feed flow rate was 100 mL min^{-1}. The gas flows were controlled and measured by calibrated mass flow controllers (Brooks). The reaction temperature was measured with a K-type thermocouple in contact with the catalyst bed. The temperature range was varied from 0 to 150 °C. The products were analyzed with a gas chromatograph Varian CP-3800 using a SUPELCO CARBOXEN 1010 PLOT 30 m × 0.53 mm column and FID and TCD detectors. All lines and valves were kept at 120 °C to prevent condensation of water vapor.

Prior to the reaction, the catalysts were dried under 30 mL min^{-1} of He flow at 150 °C for 30 min and then reduced under 30 mL min^{-1} of H$_2$ flow at 300 °C for 30 min. After the temperature was decreased to the desired reaction temperature, the reactant gas mixture was introduced to start the reaction.

The conversions of CO (X$_{CO}$) and O$_2$ (X$_{O_2}$) and the selectivity (S) of CO were calculated as:

$$X_{CO} = \frac{[CO]_{in} - [CO]_{out}}{[CO]_{in}} \times 100$$

$$X_{O_2} = \frac{[O_2]_{in} - [O_2]_{out}}{[O_2]_{in}} \times 100$$

$$S = 0.5 \times \frac{[CO]_{in} - [CO]_{out}}{[O_2]_{in} - [O_2]_{out}} \times 100$$

3. Results and discussion

3.1. BET surface area

Table 1 shows the BET surface area and pore volume of the samples. The BET surface area of the Al$_2$O$_3$ support was 240 m^2 g$_{cat}^{-1}$, which is quite similar to that of the samples, 243–250 m^2 g$_{cat}^{-1}$. This result indicates that the catalyst preparation procedure has not changed the textural properties of Al$_2$O$_3$.

3.2. Temperature programmed reduction (TPR)

Fig. 1 shows the TPR profiles for Au, Cu and Au–Cu catalysts. The TPR profile for 1%Cu/Al$_2$O$_3$ presented reduction peaks at 290 and 385 °C, the first peak due to the partial reduction of Cu^{2+} ions present in highly dispersed copper oxide species generating Cu^{1+} ions, while the second peak is ascribed to the reduction to Cu^{1+} ions to metallic copper [23–25]. The TPR profile for 2.5%Au/Al$_2$O$_3$ showed a hydrogen uptake at 190 °C ascribed to Au$_2$O$_3$ reduction [26,27]. The bimetallic sample 2.5%Au–0.5%Cu/Al$_2$O$_3$ profile showed the reduction of copper and gold oxides at one peak centered at 240 °C, probably due to Au and Cu interaction, suggesting the existence of Au–Cu bimetallic particles [19]. The TPR profiles of the 2.5%Au–1.0%Cu/Al$_2$O$_3$ and 2.5%Au–2.5%Cu/Al$_2$O$_3$ samples showed a hydrogen uptake at 200 °C due to both CuO and Au$_2$O$_3$

Table 1
BET surface area and pore volume.

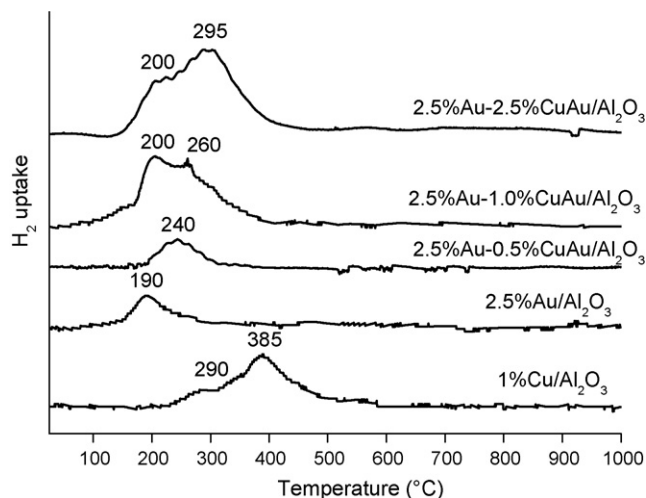| Catalyst	BET surface area (m^2 g^{-1})	Pore volume (cm^3 g^{-1})
Al$_2$O$_3$	240	0.60
2.5%Au/Al$_2$O$_3$	243	0.59
2.5%Au–0.5%Cu/Al$_2$O$_3$	250	0.60
2.5%Au–1.0%Cu/Al$_2$O$_3$	244	0.59
2.5%Au–2.5%Cu/Al$_2$O$_3$	243	0.60

Fig. 1. Temperature programmed reduction of Au–Cu/Al$_2$O$_3$ catalysts.

reduction and also showed hydrogen uptakes at 260 and 295 °C probably due to CuO and Cu$_2$O reduction not interacting with gold.

3.3. UV–vis diffuse reflectance spectroscopy (UV–vis DRS)

Fig. 2 shows the UV–vis DRS spectra of the samples. The samples did not show the plasmon absorption band between 500 and 550 nm, indicating that gold particles are not large [15,28]. The plasmon resonance of gold metal particles in the range 500–550 nm is ascribed to a collective of conduction electrons in response to optical excitation and is related to the formation of large gold particles [29]. Small gold particles show activity for CO oxidation [9]. Thus, these samples should be active during the activity tests.

The 2.5%Au/Al$_2$O$_3$ sample showed an absorption band around 280 nm in the typical region for the charge transfer transitions of Au^{3+} and Au$^+$ ions with ligands or for the absorption bands due to transition of electrons between molecular orbitals of the few-atomic clusters Au$_n$ ($n < 10$) [29].

The 1%Cu/Al$_2$O$_3$ sample showed a strong absorption band around 260 nm ascribed to (Cu$^{2+} \leftarrow$ O^{2-}) charge transfer [30–32].
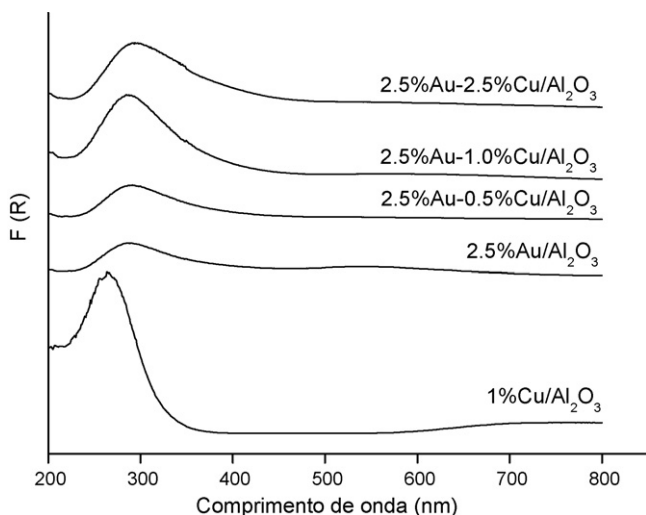

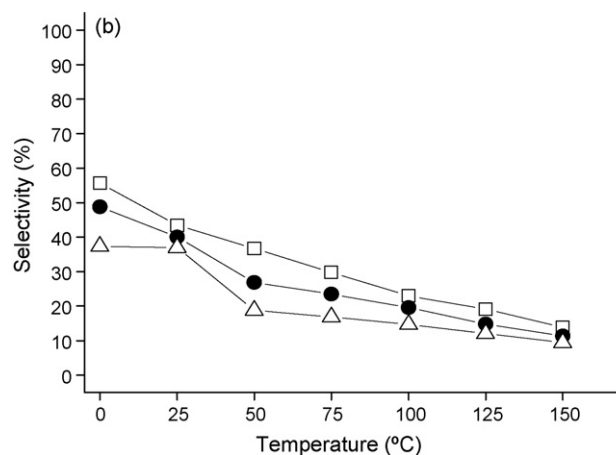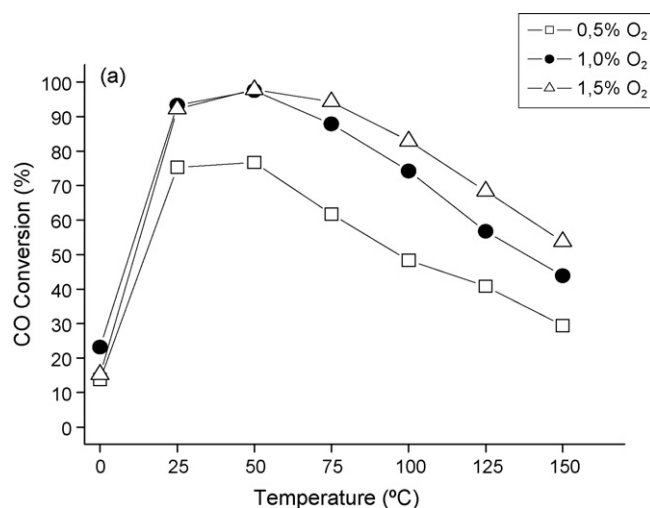**Fig. 2.** UV–vis DRS spectra of Au–Cu/Al$_2$O$_3$ catalysts.

Fig. 3. Effect of O$_2$ content on the CO conversion (a) and selectivity (b) for 2.5%Au–0.5%Cu/Al$_2$O$_3$. Reaction conditions: 50%H$_2$; 1%CO; 0.5–1.5%O$_2$; He balance; 100 mL min^{-1}, 200 mg of catalyst.

The DRS spectra of Au–Cu bimetallic samples showed one absorption band around 280 nm due to both gold and copper ion contribution.

3.4. Effect of O$_2$ content on selective CO oxidation

Fig. 3 shows the effect of O$_2$ content in the feed stream on the CO conversion and selectivity for 2.5%Au–0.5%Cu/Al$_2$O$_3$ catalyst. The O$_2$ content was varied from 0.5% to 1.5%, while the CO concentration was kept constant and equal to 1.0%. The employment of 1% of O$_2$ increased substantially the CO conversion as compared to the stoichiometric quantity of 0.5% O$_2$. Additionally, the catalytic selectivity showed a small decrease, indicating that H$_2$ oxidation also increased when an excess of O$_2$ was used. Further, increasing the O$_2$ content to 1.5% (three times the stoichiometric content for 1% of CO), the CO conversion increased again but there was an additional decrease in the selectivity. It is not recommended to use more than 1% of O$_2$ because the increase in the CO conversion would not be high enough to compensate the decrease in the selectivity. Similar results were obtained by Manasilp and Gulari [4] for Pt/Al$_2$O$_3$ catalysts. Therefore, the use of CO/O$_2$ ratio equal to 1 was more appropriate, as the CO conversion increased significantly and there was only a small decrease in the selectivity. This way, the following experiments were conducted with 1% of O$_2$ in the feed stream.
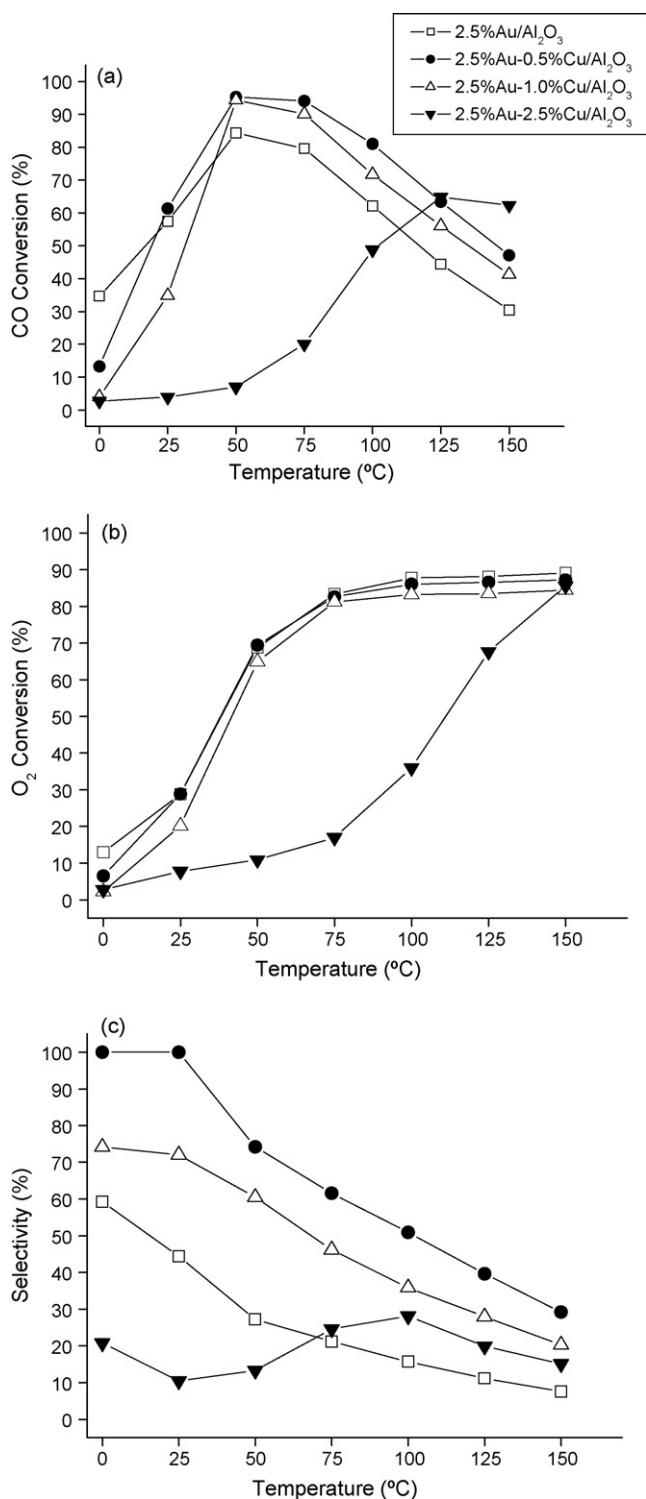
Fig. 4. Selective CO oxidation on Au–Cu/Al_2O_3 catalysts: (a) CO conversion; (b) O_2 conversion and (c) CO_2 selectivity; reaction conditions: 30%H_2; 1%O_2; 1%CO; 20%CO_2; 10%H_2O; He balance; 100 mL min^{-1}, 200 mg of catalyst.

3.5. Effect of the addition of Cu to Au/Al_2O_3 on selective CO oxidation

Fig. 4 shows the effect of Cu addition to Au catalysts on the selective CO oxidation. CO_2 and H_2O were the only products observed. The presence of CH_4 in the exit stream was not detected, which indicates methanation reaction has not occurred over the catalysts.

Methanation of CO and CO_2 occurs at higher temperatures and was observed for Ru catalysts [33]. The 2.5%Au/Al_2O_3 catalyst showed ca. 85% of CO conversion and 30% of selectivity at 50 °C. When the reaction temperature increased from 0 to 50 °C, the CO conversion raised from 35% to 85% due to an increase in the reaction rate with the temperature Above 50 °C, the CO conversion and the selectivity decreased. According to Grisel and co-workers [9], at temperatures above 50 °C the surface coverage of CO becomes so low that it no longer poisons H_2 oxidation. The decrease of the selectivity with increasing temperature indicates higher apparent activation energy for the H_2 oxidation than for the CO oxidation, which would favor H_2 oxidation as compared to CO oxidation at higher temperature [2].

The 2.5%Au/Al_2O_3 catalyst showed a high CO conversion due to the catalytic activity of Au nanoparticles. Similar results were also observed by Ko et al. [34] and Grisel and Nieuwenhuys [9] for Au/Al_2O_3. Haruta [35] showed that gold-based catalysts are extremely active in the oxidation of carbon monoxide, if gold is present as nanoparticles on a support. The DRS UV–vis spectra of our samples did not show showed any "plasmon" band, what indicates the presence of small gold particles. The active site for CO oxidation on Au/Al_2O_3 proposed by Costello and co-workers is an ensemble consisting of a cationic Au$^+$ with a hydroxyl ligand and neighboring metallic Au atoms. They suggested that the reaction occurred via the insertion of CO into Au^I–OH bonds to form hydroxycarbonyl species, which could be oxidized to give bicarbonate species. These species were proposed to undergo decarboxylation to regenerate the Au^I–OH bonds and complete the catalytic cycle [13,36,37]. In this model, the presence of metallic Au is necessary to activate the oxygen molecule, and an Au cation with a hydroxyl ligand is responsible for the conversion of CO to CO_2.

The beneficial effect of the addition of inert metal to a group VIII metal was thoroughly investigated due to the successful use of bimetallic catalysis in hydrocarbon processing [38–40]. The promoter effect was explained by changes in the electronic or geometric properties leading to higher selectivity and stability of the catalysts. The application of this idea to gold catalysts would be able to improve the properties of gold catalysts [41]. In this work, the addition of 0.5 and 1.0 wt% of copper to 2.5%Au/Al_2O_3 increased the CO conversion at temperatures higher than 50 °C (Fig. 4), although the Cu/Al_2O_3 catalyst was not significantly active in the conditions tested. In the case of Au–Cu/NaY catalysts [42], the interaction of gold with copper facilitated the activation of sites at low temperatures due to change of redox and electronic properties of gold species. Our results show that gold species with strong interaction with copper ions are active in CO oxidation at low temperature. The copper addition increased substantially the selectivity in all temperature range. This may be explained by the concept of geometric effect for bimetallic catalysts [39], which would cause a decrease on the ability of gold atoms to adsorb H_2. The 2.5%Au–0.5%Cu/Al_2O_3 catalyst showed the best behavior as compared to the other samples. Chimentão et al. [19] suggested that when copper is alloyed with gold, a net transfer of electrons is expected from copper to gold, thus, rendering copper deficient in electrons, and this is consistent to the fact that Au is more electronegative than Cu [43]. The picture is not simple, however, as there is a depletion of d-electrons charge of Au atoms, which is compensated by an increase in the conduction charge (mainly 6s orbital) [43]. Because of electron transfer due to the interaction of nanosized clusters, gold particles may become enriched in valence electron density, thereby altering the interaction of the active sites with the functional group and facilitating a partial transfer of electron density to the π* orbital of the CO bond. On the other hand, the addition of higher copper contents (1.0 and 2.5 wt%) decreased the CO conversion at low temperature. In particular, the addition of 2.5 wt% of copper seemed to block
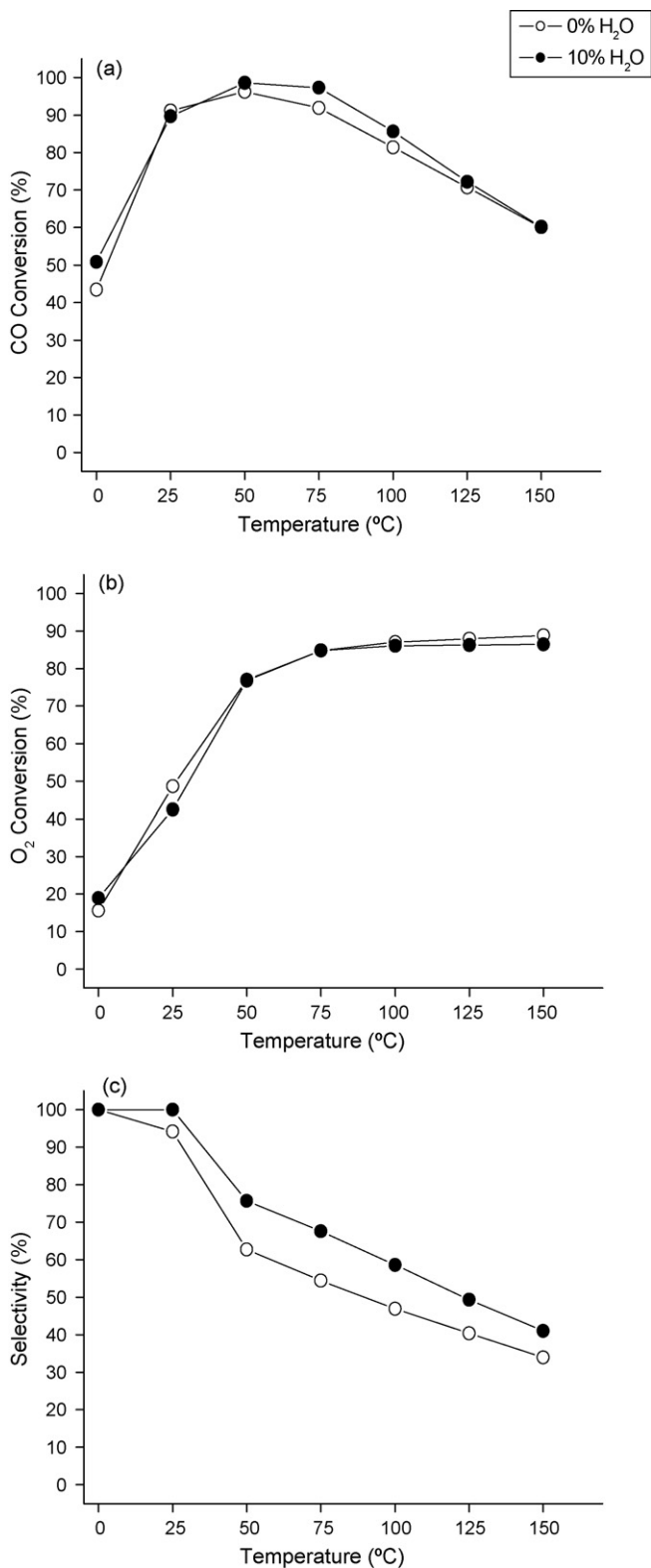
Fig. 5. Effect of the presence of H_2O in the feed stream on the CO conversion (a), O_2 conversion and selectivity (c) for 2.5%Au–0.5%Cu/Al$_2$O$_3$. Reaction conditions: 30%H_2; 1%O_2; 1%CO; 10%H_2O; He balance; 100 mL min^{-1}, 200 mg of catalyst.
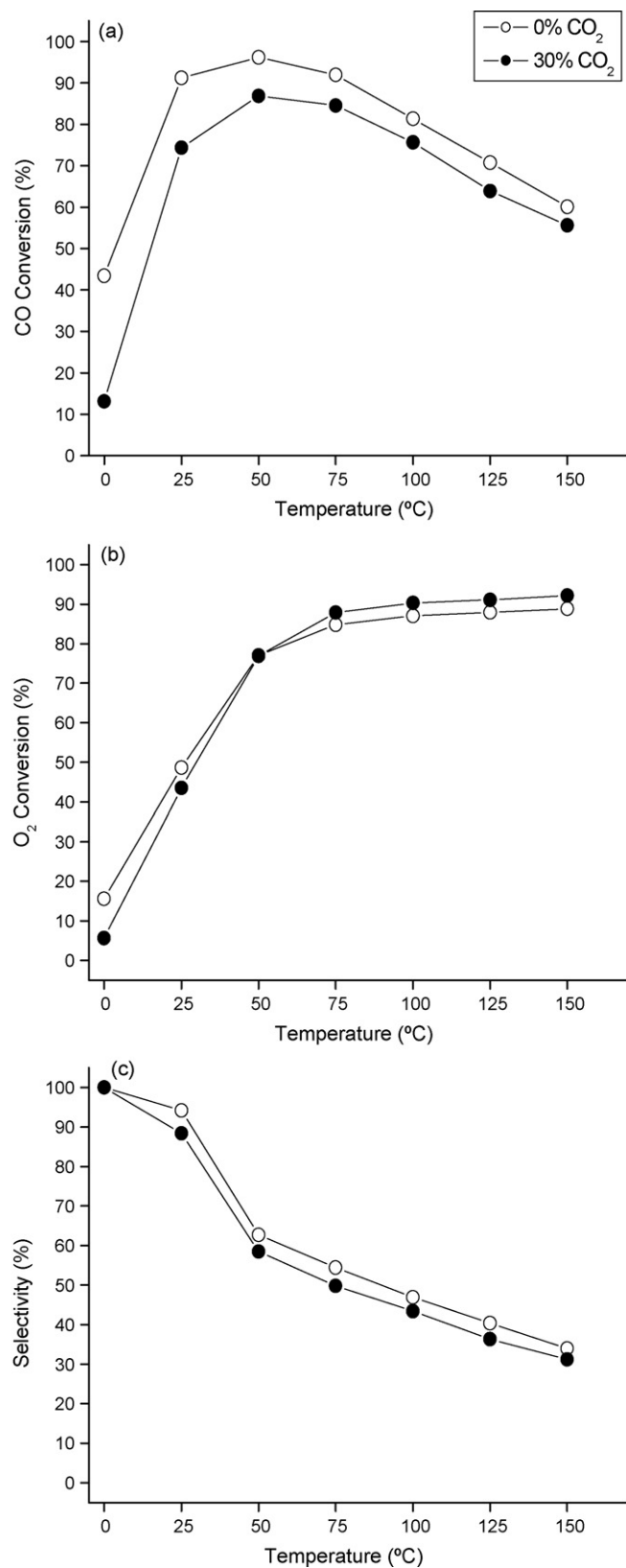
Fig. 6. Effect of the presence of CO_2 in the feed stream on the CO conversion (a), O_2 conversion and selectivity (c) for 2.5%Au–0.5%Cu/Al$_2$O$_3$. Reaction conditions: 30%H_2; 1%O_2; 1%CO; 30%CO_2; He balance; 100 mL min^{-1}, 200 mg of catalyst.

gold active sites for CO oxidation decreasing the CO conversion and impacting negatively the catalyst behavior. The O_2 conversion for 2.5%Au–2.5%Cu/Al_2O_3 catalyst was also decreased due to higher copper content, what is consistent with the hypothesis of gold sites blockage by the presence of copper.

3.6. Effect of the presence of H_2O

Fig. 5 shows the influence of the presence of 10% of water vapor in the feed stream on the behavior of 2.5%Au–0.5%Cu/Al_2O_3. A small increase in the CO conversion was observed when water vapor was present, reaching almost 100% of CO conversion at 50 °C. At this temperature, the CO conversion was maximum while the selectivity increased from 60% to 75%, and also, the selectivity was enhanced over the entire temperature range. The competitive oxidation of H_2 was suppressed by adding water vapor in the feed stream while the CO oxidation was promoted.

The beneficial effect for selective CO oxidation reaction is not due to the increase in water gas shift reaction. The low temperature water gas shift occurs at 200–400 °C while the high temperature water gas shift occurs at 400–500 °C [44]. The temperature range used during the catalyst tests was below 150 °C, where the water gas shift reaction is negligible [45]. Experimentally, it was not possible to measure the H_2 and H_2O concentrations accurately enough to be able to determine the existence and extension of water gas shift reaction in this condition.

According the model of active site for selective CO oxidation on Au/γ-Al_2O_3 catalyst proposed by Costello et al. [13] the CO oxidation occurs by the CO insertion in the Au–OH group, forming the Au–COOH species. The presence of water would avoid the dehydroxilation of the active site (2Au–OH → Au–O–Au + H_2O). This result is consistent to the beneficial water effect reported by Pansare et al. [46].

3.7. Effect of the presence of CO_2

Fig. 6 shows the effect of the addition of 30% of CO_2 in the feed stream on the selective CO oxidation. The presence of CO_2 decreased the CO conversion and also the selectivity. The CO conversion was 95% at 50 °C and diminished to 85% when 30% of CO_2 was added, while the selectivity was lower over the whole temperature range, but less affected. The O_2 conversion was quite unaffected when CO_2 was present.

The CO_2 presence decreased the CO oxidation rate due to deactivation of active sites. This deactivation is known and attributed to formation of carbonates ($CO_3{}^{2-}$) and carboxylates ($CO_2{}^-$) on the catalyst surface. The build-up carbonates species has been identified as a main source for the deactivation of gold catalysts during selective CO oxidation, most likely by blocking the Au–metal oxide surface [47]. This would explain why the selectivity is not strongly affected as both H_2 and CO_2 activities would be decreased.

According to Bollinger and Vannice [48] CO_2 and CO have a competitive adsorption on Au particles that decreases the surface coverage of CO and results in a reversible inhibitory effect on CO oxidation. As adsorbed CO_2 is an electron acceptor, the adsorption of CO_2 near to CO adsorbed on gold sites may cause an decrease in the electron density of Au sites, leading to a decrease in the CO oxidation activity [49].
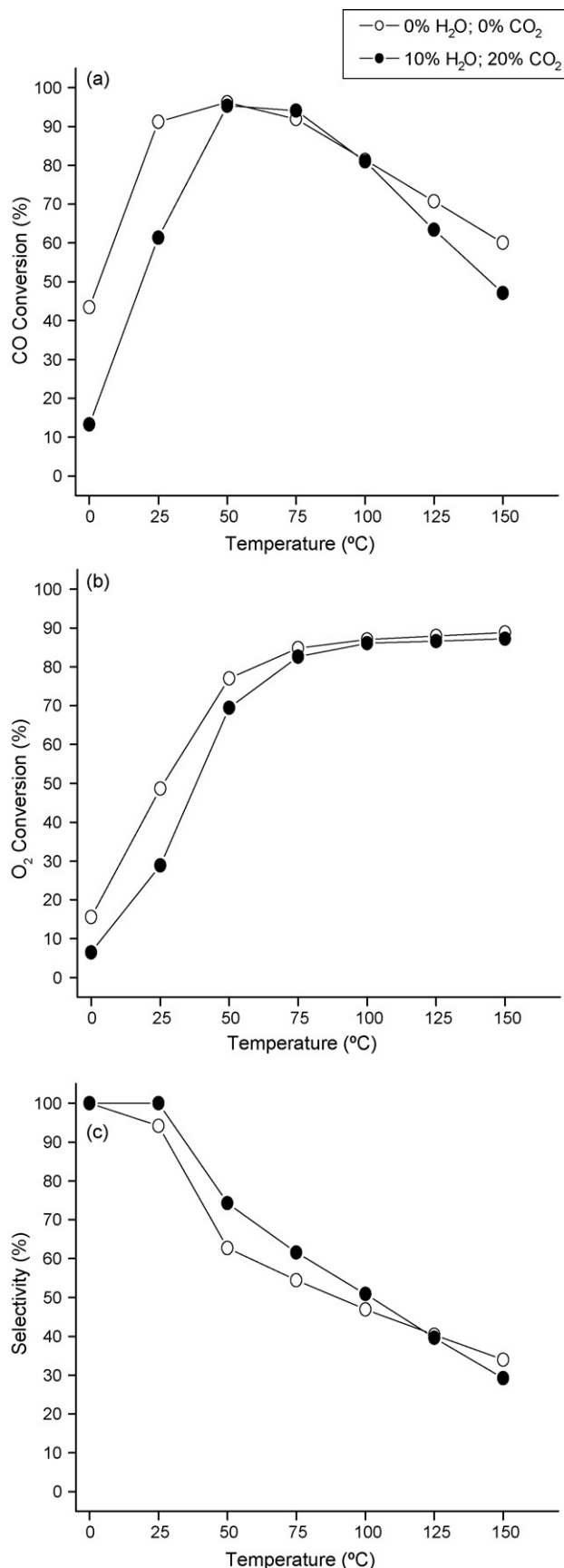

Fig. 7. Effect of the presence of H_2O and CO_2 in the feed stream on the CO conversion (a), O_2 conversion and selectivity (c) for 2.5%Au–0.5%Cu/Al_2O_3. Reaction conditions: 30%H_2; 1%O_2; 1%CO; 10%H_2O; 30%CO_2; He balance; 100 mL min⁻¹, 200 mg of catalyst.

3.8. Effect of the presence of H_2O and CO_2

Fig. 7 shows the results comparing SELOX reaction of an idealized reformate (without H_2O and CO_2) with a realistic condition (10% H_2O and 20% CO_2). When the temperature increased, the selectivity decreased faster when H_2O and CO_2 were present. In the presence of H_2O and CO_2, the O_2 conversion was lower, the CO conversion was lower but not in the whole temperature range, at 50; 75 and 100 °C the CO conversion was quite similar in the absence of H_2O and CO_2.

The presence of H_2O and CO_2 influenced CO oxidation. The deactivation due to carbonate formation in the presence of CO_2 probably was responsible for the decrease in CO and O_2 conversions. In other hand, the presence of H_2O possibly caused the regeneration of the active sites for CO oxidation by the reaction: $Au–CO_3–Au + H_2O \rightarrow Au–CO_3H + Au–OH$. The regeneration of the Au–OH active site favored only the CO oxidation and was reflected in an increase in catalytic selectivity.

Based on in situ IR data, Schubert et al. [49] reported that these effects of H_2O and CO_2 are at least partly caused by coadsorption of CO_2 and/or H_2O/OH species on the gold particles or at the Au-oxide interface. The built-up and accumulation of carbonate by-products is manly related to catalyst deactivation. These species can be thermally transformed into less stable bicarbonate species by the presence of H_2O, which reduces the tendency for deactivation. The counteracting effects of both H_2O and CO_2 under a realistic application may or not able to compensate each other leading to a small decreases in the catalytic activity depending on the temperature of the reaction.

4. Conclusions

Bimetallic Au–Cu catalysts were prepared by the deposition–precipitation method. This method generated small gold particles, as identified by the absence of plasmon absorption band in the DRS UV–vis spectra. The effect of Cu addition was verified in different contents: 0.5, 1.0 and 2.5 wt%. The results of selective CO oxidation reaction showed that Cu addition increased the selectivity for CO oxidation decreasing the H_2 consumption. The interaction between Cu and Au seemed to be able to modify the catalytic properties of Au active sites for CO oxidation. There is an optimal Cu content to benefit the CO oxidation, as high contents of copper lead to blocking of gold active sites. The increase in the O_2 content from 0.5% to 1% increased substantially the CO conversion although it was followed by a slightly decrease in the selectivity. The effect of H_2O and CO_2 were studied, simulating a realistic condition for SELOX on 2.5%Au–0.5%Cu/Al$_2$O$_3$ catalyst. The presence of H_2O was beneficial, providing an increase in the CO conversion and also a small increase in the selectivity. However, the presence of CO_2 decreased the CO conversion and selectivity. In a realistic experimental where both H_2O and CO_2 are present the CO conversion was not affected in the temperature of maximum conversion at 50 °C and the catalyst was more selective.

Acknowledgements

References

[1] A. Stambouli, E. Traversa, Renew. Sustain. Energy Rev. 6 (2002) 295.
[2] G. Avgouropoulos, T. Ioannies, C. Papadopolou, J. Batista, S. Hocevar, H.K. Matralils, Catal. Today 75 (2002) 157.
[3] Y. Tanaka, T. Utaka, R. Kikuchi, K. Sasaki, Appl. Catal. A: Gen. 238 (2003) 11.
[4] A. Manasilp, E. Gulari, Appl. Catal. B: Environ. 37 (2002) 17.
[5] A. Luengnaruemitchai, S. Osuwan, E. Gulari, Int. J. Hydrogen Energy 29 (2004) 429.
[6] P. Marques, N.F.P. Ribeiro, M. Schmal, D.A.G. Aranda, M.M.V.M. Souza, J. Power Sources 158 (2006) 504.
[7] M. Haruta, T. Kobayashi, H. Sano, N. Yamada, Chem. Lett. 16 (1987) 405.
[8] R.M.T. Sanchez, A. Ueda, K. Tanaka, M. Haruta, J. Catal. 168 (1997) 125.
[9] R.J.H. Grisel, B.E. Nieuwenhuys, J. Catal. 199 (2001) 48.
[10] M. Haruta, M. Date, Appl. Catal. A: Gen. 222 (2001) 427.
[11] E.D. Park, J.S. Lee, J. Catal. 189 (1999) 1.
[12] J.C. Fierro-Gonzalez, J. Guzman, B.C. Gates, Top. Catal. 44 (2007) 103.
[13] C.K. Costello, M.C. Kung, H.-S. Oh, Y. Wang, H.H. Kung, Appl. Catal. A: Gen. 232 (2002) 159.
[14] T.V. Choudhary, D.W. Goodman, Appl. Catal. A: Gen. 291 (2005) 32.
[15] G.K. Bethke, H.H. Kung, Appl. Catal. A: Gen. 194 (2000) 43.
[16] B. Hvolbæk, T.V.W. Janssens, B.S. Clausen, H. Falsig, C.H. Christensen, J.K. Nørskov, Nano Today 2 (2007) 14.
[17] A.C. Gluhoi, B.E. Nieuwenhuys, Catal. Today 122 (2007) 226.
[18] S. Monyanona, S. Pongstabodeea, A. Luengnaruemitchai, J. Power Sources 163 (2006) 547.
[19] R.J. Chimentão, F. Medina, J.L.G. Fierro, J. Llorca, J.E. Sueiras, Y. Cesteros, P. Salagre, J. Mol. Catal. A: Chem. 274 (2007) 159.
[20] X. Liu, A. Wang, X. Wang, C. Mou, T. Zhang, Chem. Commun. 27 (2008) 3187.
[21] H.H. Kung, M.C. Kung, C.K. Costello, J. Catal. 216 (2003) 425.
[22] H.-S. Oh, J.H. Yang, C.K. Costello, Y.M. Wang, S.R. Bare, H.H. Kung, M.C. Kung, J. Catal. 210 (2002) 375.
[23] B.M. Nagaraja, V. Siva Kumar, V. Shashikala, A.H. Padmasri, S. Sreevardhan Reddy, B. David Raju, K.S. Rama Rao, J. Mol. Catal. A: Chem. 223 (2004) 339.
[24] F.M.T. Mendes, M. Schmal, Appl. Catal. A: Gen. 151 (1997) 393.
[25] A.J. Rouco, Appl. Catal. A: Gen. 117 (1994) 139.
[26] A. Wolf, F. Schuth, Appl. Catal. A: Gen. 226 (2002) 1.
[27] G. Neri, A.M. Visco, S. Galvagno, A. Donato, M. Panzalorto, Thermochim. Acta 329 (1999) 39.
[28] R. Zanella, S. Giorgio, C.-H. Shin, C.R. Henry, C. Louis, J. Catal. 222 (2004) 357.
[29] I. Tuzovskaya, N. Bogdanchikova, A. Simakov, V. Gurin, A. Pestryakov, M. Avalos, M.H. Farías, Chem. Phys. 338 (2007) 23.
[30] H. Praliaud, S. Mikhailenko, Z. Chajar, M. Primet, Appl. Catal. B: Environ. 16 (1998) 359.
[31] D. Paket, W. Dehertogh, R.A. Schoonheydt, in: B. Drzaj, S. Hocevar, S. Pejovnik (Eds.), Zeolites, Elsevier, Amsterdam, 1985.
[32] H. Praliaud, Y. Kadratoff, G. Coudurier, M.V. Mathieu, Spectrochim. Acta Part A 30 (1974) 1389.
[33] T. Utaka, T. Takeguchi, R. Kikuchi, K. Eguchi, Appl. Catal. A: Gen. 246 (2003) 117.
[34] E.-Y. Ko, E.D. Park, K.W. Seo, H.C. Lee, D. Lee, S. Kim, Catal. Today 116 (2006) 377.
[35] M. Haruta, Catal. Today 36 (1997) 153.
[36] C.K. Costello, J.H. Yang, H.Y. Law, Y. Wang, J.-N. Lin, L.D. Marks, M.C. Kung, H.H. Kung, Appl. Catal. A: Gen. 243 (2003) 15.
[37] H.C. Fierro-Gonzalez, B.C. Gates, Catal. Today 122 (2007) 201.
[38] J.H. Sinfelt, Bimetallic Catalysts: Discoveries, Concepts and Applications, Wiley, New York, 1983.
[39] V. Ponec, Adv. Catal. 32 (1983) 149.
[40] H. Verbeek, W.M.H. Sachtler, J. Catal. 25 (1972) 350.
[41] A.C. Gluhoi, S.D. Lin, B.E. Nieuwenhuys, Catal. Today 90 (2004) 175.
[42] E. Smolentseva, N. Bogdanchikova, A. Simakov, A. Pestryakov, I. Tusovskaya, M. Avalos, M.H. Farías, J.A. Díaz, V. Gurin, Surf. Sci. 600 (2006) 4256.
[43] M. Kuhn, T.K. Sham, Phys. Rev. B 49 (1994) 1647.
[44] A. Luengnaruemitchai, S. Osuwan, E. Gulari, Catal. Commun. 4 (2003) 215.
[45] G. Avgouropoulos, T. Ioannides, Ch. Papadopoulou, J. Batista, S. Hocevar, H.K. Matralis, Catal. Today 75 (2002) 157.
[46] S.S. Pansarea, A. Sirijaruphanb, J.G. Goodwin Jr., J. Catal. 234 (2005) 151.
[47] M. Schubert, V. Plzak, J. Garche, J. Behm, Catal. Lett. 76 (3/4) (2001) 143.
[48] M.A. Bollinger, M.A. Vannice, Appl. Catal. B: Environ. 8 (1996) 417.
[49] M. Schubert, A. Venugopal, M.J. Kahlich, V. Plzak, J. Behm, J. Catal. 222 (2004) 32.